

The Landau gauge gluon propagator: Gribov problem and finite-size effects*

I. L. Bogolubsky

Joint Institute for Nuclear Research, 141980 Dubna, Russia
E-mail: bogolubs@jinr.ru

V. G. Bornyakov

Institute for High Energy Physics, 142281 Protvino, Russia
Institute for Theoretical and Experimental Physics, 117259 Moscow, Russia
E-mail: vitaly.bornyakov@ihep.ru

G. Burgio[†]

Universität Tübingen, Institut für Theoretische Physik, 72076 Tübingen, Germany
E-mail: burgio@tphys.physik.uni-tuebingen.de

E.-M. Ilgenfritz, M. Müller-Preussker[‡], P. Schemel

Humboldt-Universität zu Berlin, Institut für Physik, 12489 Berlin, Germany
E-mail: ilgenfri@physik.hu-berlin.de,
mmp@physik.hu-berlin.de, peter.schemel@mathematik.hu-berlin.de

V.K. Mitrjushkin

Joint Institute for Nuclear Research, 141980 Dubna, Russia
Institute for Theoretical and Experimental Physics, 117259 Moscow, Russia
E-mail: vmitr@theor.jinr.ru

The $SU(2)$ gluon propagator in Landau gauge is studied on the lattice. Our gauge fixing procedure employs simulated annealing and $\mathbb{Z}(2)$ -flips. It finds higher maxima of the gauge functional compared with those obtained with the standard overrelaxation and leads to systematic deviations of the gluon propagator in the infrared region. In particular, finite-size effects for lattice sizes from $(1.7 \text{ fm})^4$ up to $(6.5 \text{ fm})^4$ become weak. The propagator shows a plateau at $p \approx 300 \text{ MeV}$.

The XXV International Symposium on Lattice Field Theory
July 30 - August 4, 2007
Regensburg, Germany

*This work was supported by the DFG under contracts FOR 465 / Mu 932/2-4 and 436 RUS 113/866 as well as by the RFBR-DFG grant 06-02-04014.

[†]Supported under contract DFG Re856/6-1,2.

[‡]Speaker.

1. Introduction

Over the years, considerable progress has been made in solving non-perturbative Dyson-Schwinger equations (DSE) for gauge-variant Green functions, in particular for the covariant Landau gauge (for a recent review see [1]). Besides the interest in the DSE solutions as input for Bethe-Salpeter or Faddeev bound state equations, their infrared asymptotics is of importance for a check for gluon and quark confinement scenarios proposed by Gribov [2] and Zwanziger [3] on one hand and Kugo-Ojima [4] on the other. These scenarios claim confinement to be intimately connected with a Landau gauge ghost propagator diverging and with a gluon propagator vanishing in the zero-momentum limit. Such a behavior has been realized with asymptotic power-type solutions of (truncated) DSE with infrared exponents leading necessarily to a running coupling constant with a non-trivial infrared fixed point [5]. This behavior has been confirmed independently by studies of exact renormalization group equations [6] and with stochastic quantization [7]. Recently it has been even argued that a unique and exact power-like infrared asymptotic behavior of all Green functions can be derived without truncating the hierarchy of DSE [8]. However, in order to interpolate the full momentum dependence from the infrared to the perturbative ultraviolet regime, one still has to rely on truncations which are hard to control. Very recently, solutions of the truncated system studied on a finite torus have been presented with a specific finite-size dependence which smoothly turns into the exact power-like infrared behavior at infinite volume [9].

This gives us a good motivation to compare with the ab-initio non-perturbative path integral approach approximated on a Euclidean four-dimensional lattice. The lattice approach has its own limitations. Numerical simulations can be carried out only on a finite lattice. Therefore, for large momenta close to the inverse lattice spacing we shall encounter discretization effects, whereas at low momenta we are faced with the limitations of the finite volume as well as with rotational symmetry violations due to the hypercubic lattice geometry. Moreover, gauge fixing is not unique resulting in the so-called *Gribov problem*. It has been argued that the gauge copy dependence should disappear in the infinite-volume limit if the copies are bounded to the *Gribov region* - the positivity region of the Faddeev-Popov operator [10]. But on a finite lattice, Gribov copy effects may influence the infrared asymptotics and therefore, at least partly, be responsible for finite-size effects. Standard algorithms like overrelaxation (OR) find always local extrema of the gauge functional. Repeating such an algorithm with random initial gauges one can find better extrema coming closer to or eventually finding *the* global maximum - *i.e.* elements of the *fundamental modular region*. We call the copy found after a number of trials which guarantees stable values of the gauge functional, at least in the statistical average, the *best copy* (bc) to be compared e.g. with the *first copy* (fc). The gauge transformations determined in these gauge fixing procedures are normally restricted to be periodic. Under these circumstances for the Landau gauge the bc ghost propagator has been shown to deviate up to 10% from fc results, whereas the gluon propagator did not differ within statistical errors [11, 12].

In this contribution we present an improved gauge fixing method which allows to reach considerably higher extrema of the gauge functional than the above mentioned bc OR method. In the simpler case of $SU(2)$ we shall demonstrate the gluon propagator to become influenced and to have a weaker volume dependence in the infrared. We hope that this method will allow to check in the near future whether the gluon propagator really has the chance to tend to zero in the infrared limit.

The new method relies first on a systematic use of the simulated annealing (SA) algorithm with subsequent finalizing OR to maximize the gauge functional and second on an enlargement of the gauge orbits by special non-periodic (modulo elements of the center $\mathbb{Z}(2)$) gauge transformations, representing an exact (unbroken) symmetry of the local gauge action. First results obtained with this method were reported in [13, 14]. Restricting ourselves to the infrared region we present gluon propagator results here only for one considerably strong bare coupling value $\beta \equiv 4/g_0^2 = 2.20$. The corresponding lattice scale a is fixed with the string tension $\sigma = (440 \text{ MeV})^2$ adopting $\sqrt{\sigma}a = 0.469$ [15]. Thus, our largest lattice size 32^4 corresponds to a volume $(6.5 \text{ fm})^4$.

2. Improved gauge fixing

Landau gauge fixing is equivalent to maximizing the gauge functional of a given lattice field $\{U\}$

$$F_U[g] = \frac{1}{4L^4} f_U[g], \quad f_U[g] = \sum_{x,\mu} \frac{1}{2} \text{Tr} \, {}^g U_{x\mu} \quad \text{with} \quad {}^g U_{x\mu} = g(x + \hat{\mu}) U_{x\mu} g(x)^\dagger \quad (2.1)$$

with respect to the local gauge transformation $g(x) \in SU(2)$. The SA method generates g stochastically with the Boltzmann weight $w(g) \propto \exp(-f_U[g]/T)$, where the “temperature” $T \in [T_{min}, T_{max}]$ is a technical parameter which has to be lowered (we have chosen equal temperature steps between the lattice sweeps) from a certain value T_{max} until g is locked within the region of attraction of a local maximum. For the local updates of g the heatbath algorithm is used. After having reached T_{min} , OR sweeps are employed until the lattice equivalent of $\partial_\mu A_\mu(x) = 0$ is reached at all x with a given accuracy. The more slowly the SA cooling process is chosen the higher should be the probability to reach the global maximum. The method has been very successfully applied for the first time for gauge fixing in the case of the maximally Abelian gauge in Ref. [16]. In order to see in as far the SA method (with finalizing OR) is more efficient than the only application of the OR algorithm we have selected for each gauge field $\{U\}$ up to 15 highest distinct local maxima F_i , $i = 1, 2, \dots$. On a lattice 16^4 at $\beta = 2.40$ they can be well identified with a sufficiently large number of repetitions with initial random gauges. We measured the probabilities $P(F)$ for each method to find the values $F = F_i$. The result is shown on the left of Fig. 1. We compare OR with SA, the latter for various choices of the number of temperature iteration steps. SA is clearly seen to win even with a number of $O(1000)$ iterations. An SA iteration costs more CPU time than the simpler OR sweep. Therefore, one could think a repeated application of OR to be more time efficient. On the right hand side of Fig. 1 the probability to find the overall maximum $F_1 = F_{max}$ is shown versus the average CPU time required for the given version of algorithm. We see that even with respect to the computing time SA (including finalizing OR) is more efficient to find F_{max} . We are convinced that SA becomes increasingly efficient for lower β and larger volume, respectively. Moreover, we have seen that SA is much improving, when microcanonical steps (in the following always three) are included after each iteration. In the left part of Fig. 2 we compare the probabilities $P(F)$ of OR with SA for various lower temperatures T_{min} . We have measured the performance parameter introduced in Ref. [17] and defined as $G \equiv -\log(1 - P(F_{max}))/t_r$, where t_r denotes the CPU time in arbitrary units. Corresponding estimates for G are shown in the right part of Fig. 2. For what follows we decided to apply SA with $T_{min} = 0.01$ and 1000 iterations with equal temperature steps always combined with microcanonical sweeps.

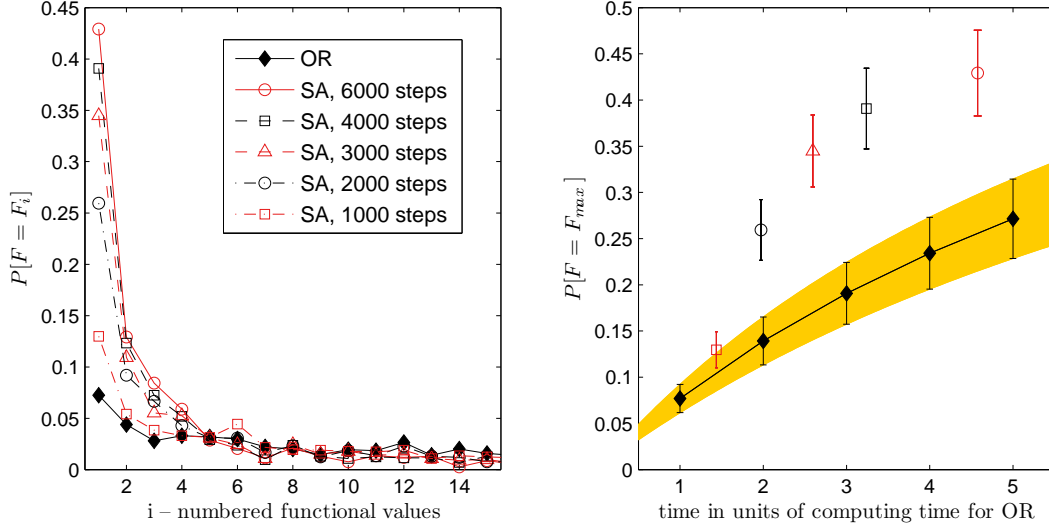


Figure 1: Left: Probability to find the gauge copy with the functional value F_i of rank $i = 1, 2, \dots$ for the SA method with a number of temperature steps varying from 1000 to 6000 (for fixed $T_{min} = 0.4$ and $T_{max} = 1.4$). For comparison we show also the result of the standard OR method with one (the “first”) random copy. **Right:** The corresponding probability to find the overall highest maximum $F_1 = F_{max}$ is shown vs. CPU time required for the SA method with varying number of temperature steps. For comparison the result for the OR method is shown when repeated with an increasing number of initial random gauges (curved line). The CPU time unit is the average time the OR method needs for one gauge copy to achieve the required accuracy of gauge fixing. 37 configurations, each with 50 gauge copies have been considered.

The second feature of our improved gauge fixing procedure are $\mathbb{Z}(2)$ flip transformations. For $SU(2)$ gauge theory, each flip transformation consists of a simultaneous $\mathbb{Z}(2)$ flip of all links $U_{x\mu} \rightarrow -U_{x\mu}$ throughout a 3D hyperplane at a given value of the coordinate x_μ . This is just a particular case of a gauge transformation which is periodic modulo $\mathbb{Z}(2)$,

$$g(x + L\hat{\mu}) = z_\mu g(x), \quad z_\mu = \pm 1 \in \mathbb{Z}(2). \quad (2.2)$$

The procedure is equivalent to search for the best sector (determined by the signs of the four averaged Polyakov loops) among $2^4 = 16$ sectors that provides the highest maximum of F . In order to decide which one is the optimal sector, the SA method has to be applied repeatedly with the aim to find the best copy within each sector. In practice the procedure can be somewhat simplified (see Ref. [14]). We will abbreviate the combined gauge fixing method as the FSA (flip-SA) algorithm.

In Table 1 we show the strong effect of the flips on the average gauge functional. $F(n_c)$ denotes the best functional value found with SA from n_c random starts in every chosen flip sector. In case “SA” we did not apply flips at all, *i.e.* the Polyakov loop sector is chosen randomly by the Monte Carlo procedure. In case “FSA” we have searched within *all* 16 flip sectors.

3. Lattice gluon propagator results

The combined FSA method, and for comparison also the standard OR method, have been applied to

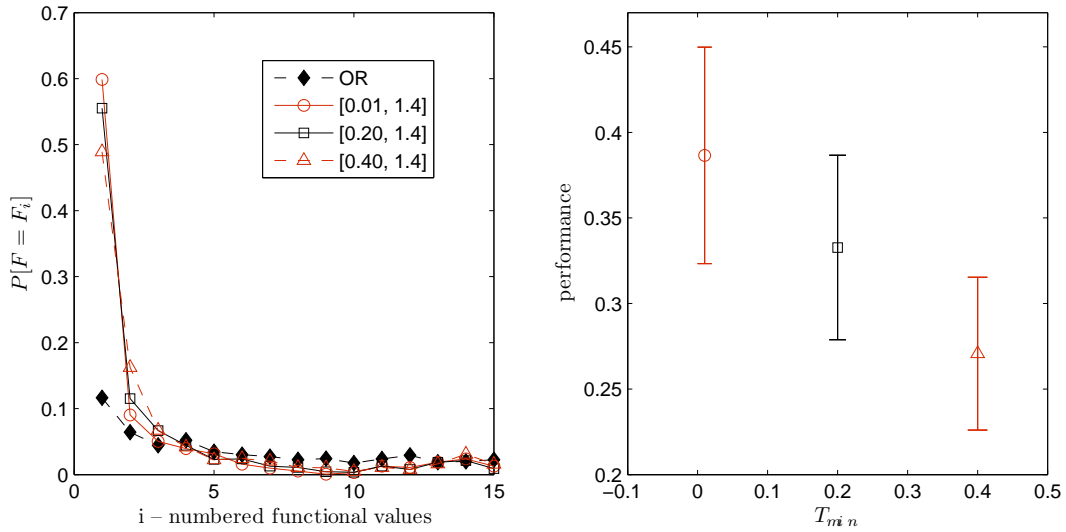


Figure 2: **Left:** Probability to find the gauge copy with the functional value F_i of rank $i = 1, 2, \dots, 15$ shown for the methods OR and SA, for the latter with varying final temperature $T_{min} = 0.01, 0.2, 0.4$ and a fixed number of 1000 temperature steps each supplied with 3 microcanonical steps ($T_{max} = 1.4$). **Right:** Performance parameter G as defined in the text for the SA method shown as function of the final temperature T_{min} . For both figures 33 configurations, each with 50 gauge copies have been considered for $\beta = 2.4$ and lattice size 16^4 .

SA / FSA	n_c	$\langle F(n_c) \rangle - F_0$ for 16^4	$\langle F(n_c) \rangle - F_0$ for 24^4
SA	1	$1(8) \cdot 10^{-5}$	$25(4) \cdot 10^{-5}$
SA	5	$6(8) \cdot 10^{-5}$	$31(4) \cdot 10^{-5}$
FSA	1	$32(9) \cdot 10^{-5}$	$36(4) \cdot 10^{-5}$
FSA	2	$33(9) \cdot 10^{-5}$	$38(4) \cdot 10^{-5}$
FSA	3	$34(9) \cdot 10^{-5}$	$38(4) \cdot 10^{-5}$
FSA	4	$34(9) \cdot 10^{-5}$	$39(4) \cdot 10^{-5}$
FSA	5	$34(9) \cdot 10^{-5}$	$39(4) \cdot 10^{-5}$

Table 1: The average gauge functionals $\langle F(nc) \rangle$ with an arbitrary value $F_0 = 0.82800$ subtracted. For the lattice sizes 16^4 and 24^4 the numbers of investigated MC configurations with $\beta = 2.20$ are 60 and 46, respectively.

the computation of the gluon propagator at momentum $p_\mu = (2/a) \sin(\pi k_\mu/L)$, $k_\mu \in (-L/2, L/2]$

$$D_{\mu\nu}^{ab}(p) = \langle \tilde{A}_\mu^a(k) \tilde{A}_\nu^b(-k) \rangle = \left(\delta_{\mu\nu} - \frac{p_\mu p_\nu}{p^2} \right) \delta^{ab} D(p), \quad (3.1)$$

where $\tilde{A}(k)$ represents the Fourier transform of the gauge potentials

$$A_\mu(x + \hat{\mu}/2) = \frac{1}{2ia g_0} (U_{x\mu} - U_{x\mu}^\dagger) \quad (3.2)$$

after the gauge has been fixed.

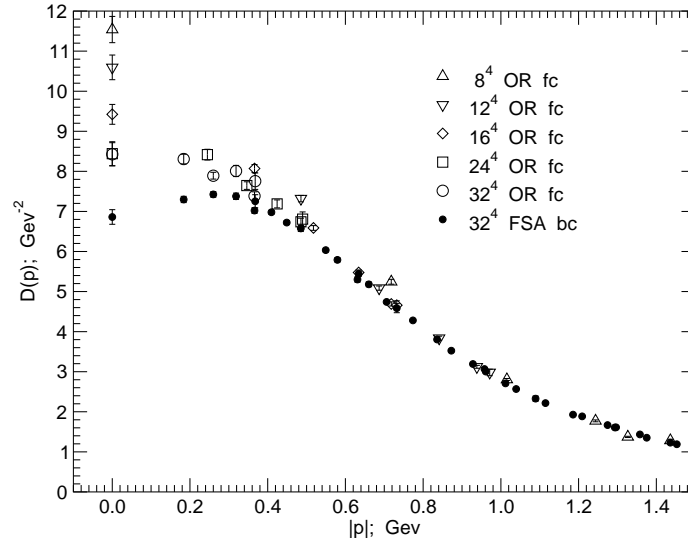


Figure 3: Gluon propagator versus momentum and the zero-momentum propagator $D(0)$, for $\beta = 2.20$ and for various lattice sizes, obtained with fc OR compared with bc FSA. The lattice size is 32^4 .

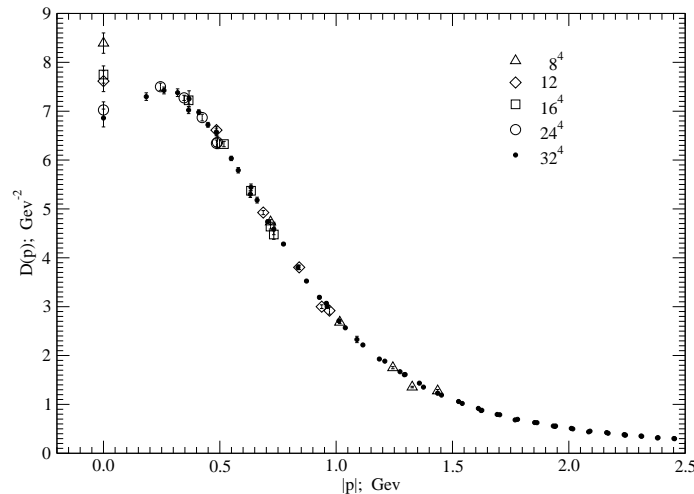


Figure 4: The gluon propagator and $D(0)$, obtained with bc FSA gauge fixing, shown in the infrared region for various lattice sizes ($\beta = 2.20$).

Fig. 3 shows the comparison of the fc OR results obtained for several lattice sizes with the bc FSA result for 32^4 only. At $p = 0$ the zero-momentum data points $D(0)$ are also plotted. The OR data exhibit quite strong finite-size effects. Contrary to the OR results the FSA data seem smoothly to extrapolate to the $D(0)$ data point. In Fig. 4 we show our bc FSA result for various lattice sizes. In comparison to OR (see Fig.3) the FSA result shows considerably less finite-size effects down to the lowest accessible momenta. All data points fall more or less onto a universal curve. This leads us to hope that the visible plateau indicates the existence of a turning point beyond which $D(p)$ starts to decrease for $p \rightarrow 0$.

4. Conclusions

In this contribution we have discussed an improved gauge fixing method which takes $\mathbb{Z}(2)$ flips into account and makes consequently use of simulated annealing to maximize the Landau gauge functional. The combined algorithm finds considerably larger functional values. It lowers the values of the gluon propagator in the infrared in comparison with the OR results. Moreover, finite-size effects seem to become suppressed. They do not show the specific behavior found with DSE on a finite torus [9]. By further increasing the lattice size we hope to see $D(p)$ to pass a maximum and to tend to smaller values in the far infrared. So far, such a behavior has been found only in the lower dimensional cases [18, 19].

References

- [1] R. Alkofer, *Braz. J. Phys.* **37** (2007) 144 [hep-ph/0611090].
- [2] V. N. Gribov, *Nucl. Phys.* **B139** (1978) 1.
- [3] D. Zwanziger, *Nucl. Phys.* **B412** (1994) 657.
- [4] T. Kugo and I. Ojima, *Prog. Theor. Phys. Suppl.* **66** (1979) 1; T. Kugo, hep-th/9511033.
- [5] L. von Smekal, R. Alkofer, and A. Hauck, *Phys. Rev. Lett.* **79** (1997) 3591 [hep-ph/9705242].
- [6] J. M. Pawłowski, D. F. Litim, S. Nedelko, and L. von Smekal, *Phys. Rev. Lett.* **93** (2004) 152002 [hep-th/0312324].
- [7] D. Zwanziger, *Phys. Rev.* **D65** (2002) 094039 [hep-th/0109224].
- [8] C. S. Fischer and J. M. Pawłowski, *Phys. Rev.* **D75** (2007) 025012 [hep-th/0609009].
- [9] C. S. Fischer, A. Maas, J. M. Pawłowski, and L. von Smekal, hep-ph/0701050.
- [10] D. Zwanziger, *Phys. Rev.* **D69** (2004) 016002 [hep-ph/0303028].
- [11] A. Cucchieri, *Nucl. Phys.* **B508** (1997) 353 [hep-lat/9705005].
- [12] A. Sternbeck, E.-M. Ilgenfritz, M. Müller-Preussker, and A. Schiller, *Phys. Rev.* **D72** (2005) 014507 [hep-lat/0506007].
- [13] I. L. Bogolubsky, G. Burgio, M. Müller-Preussker, and V. K. Mitrjushkin, *Phys. Rev.* **D74** (2006) 034503 [hep-lat/0511056].
- [14] I. L. Bogolubsky, *et al.*, arXiv:0707.3611 [hep-lat].
- [15] J. Fingberg, U. M. Heller, and F. Karsch, *Nucl. Phys.* **B392** (1993) 493–517 [hep-lat/9208012].
- [16] G. S. Bali, V. Bornyakov, M. Müller-Preussker, and K. Schilling, *Phys. Rev.* **D54** (1996) 2863 [hep-lat/9603012].
- [17] P. Schemel, *Master Thesis, Humboldt University Berlin* (2006).
- [18] A. Cucchieri, A. Maas, and T. Mendes, *Mod. Phys. Lett.* **A22** (2007) 2429 [hep-lat/0701011].
- [19] A. Maas, *Phys. Rev.* **D75** (2007) 116004 [arXiv:0704.0722 [hep-lat]].